Journal of Applied Physics ARTICLE scitation.org/journal/jap

Annular antenna array metamaterial with SINIS bolometers

Cite as: J. Appl. Phys. **125**, 174501 (2019); doi: 10.1063/1.5054160
Submitted: 30 August 2018 · Accepted: 16 April 2019 ·
Published Online: 3 May 2019

M. Tarasov,[1,a)] A. Sobolev,[1] A. Gunbina,[2] G. Yakopov,[3] A. Chekushkin,[1] R. Yusupov,[1] S. Lemzyakov,[4] V. Vdovin,[2] and V. Edelman[4]

AFFILIATIONS

[1]V. Kotelnikov Institute of Radio Engineering and Electronics RAS, 125009 Moscow, Russia
[2]Institute of Applied Physics, Russian Academy of Sciences (IAP RAS), 603950 Nizhny Novgorod, Russia
[3]Special Astrophysical Observatory, Big Altazimuth Telescope, 369167 Nizhny Arhyz, Russia
[4]P. Kapitza Institute for Physical Problems RAS, 117334 Moscow, Russia

Note: This paper is part of the Special Topic section "Advances in Terahertz Solid-State Physics and Devices" published in J. Appl. Phys. **125**(15) (2019).

[a)]tarasov@hitech.cplire.ru

ABSTRACT

We fabricated and experimentally studied a wideband metamaterial comprising a 2D array of annular antennas with Superconductor-Insulator-Normal metal-Insulator-Superconductor (SINIS) bolometers. The annular antenna array metamaterial was designed for a frequency range of 300–450 GHz and consists of periodically arranged electrically small rings, each containing two or four SINIS bolometers connected in series or parallel. These periodic structures with a unit cell size of about one-tenth of a wavelength act as a distributed absorber and receive two orthogonal polarizations. The unit's small cell size provides a higher density of bolometers and therefore increases the bandwidth and the dynamic range of a single pixel. Theoretical estimates at a central frequency of 345 GHz yield absorption efficiencies of over 80% of the incident RF power within the 300–450 GHz frequency range. The average absorption by the metamaterial matrix in the given frequency band is at least twice as high in comparison to the half-wave circle matrix. We measured the optical response at sample temperatures as low as 100 mK using a quasi-optical setup that consisted of an immersion sapphire lens, bandpass mesh filters, and a variable temperature cryogenic blackbody radiation source. The measured series array voltage responsivity was 1.3×10^9 V/W for radiation temperatures ranging from 2 K to 7.5 K. The current responsivity for the parallel array was 2.4×10^4 A/W at a bath temperature of 100 mK. The spectral response was measured in a 240–370 GHz range with a Backward Wave Oscillator radiation source. The measured equivalent temperature sensitivity could be reduced to 100 μK/Hz$^{1/2}$ at a 2.7 K radiation temperature level, a value that is suitable for anisotropy measurements in cosmic microwave background radiation.

I. INTRODUCTION

Planar antennas can match free-space radiation in different ways. Two possible approaches are (i) the use of conventional antennas with a size that corresponds to about half the wavelength of interest or (ii) the use of electrically small antennas. A typical metamaterial consists of a periodic array of subwavelength metallic resonators that are collectively coupled to the free-space excitation. With small antennas, the matrix can be designed to accommodate a wider bandwidth and occupy a much smaller physical space which allows it to be placed in the waist of a single-mode horn or in the focus of immersion lens. According to the fundamental criteria,[1] antennas whose field outside the sphere corresponds to that of an infinitesimally small dipole have potentially the broadest bandwidth of all antennas and a gain of 1.5. If the metamaterial is arranged as a periodic matrix of conducting elements, it can effectively interact with incoming radiation even when the elements' size and spacing are much smaller than half a wavelength. A well-known example of such a structure is an array consisting of split-ring antennas.[2] For such a device type, the half wavelength limitation does not apply.[3] Qualitatively, the performance of such an antenna is somewhat like

shortening the antenna through a lumped capacitor, which means that it can be treated like a lump element tank circuit. If these elements are combined into a dense matrix with strong interaction between individual elements, it is possible to achieve a rather effective interaction with radiation.[4] An absorbing metamaterial can provide nearly 100% absorbance efficiency.[5] As the size of individual metamaterial units is in the subwavelength range, it has the inherent capability to operate at the diffraction limit. Due to their capacity for enhancing electric fields and improving antenna performance, metamaterials are used in numerous applications that involve anything from optical to radio frequencies.[6] A recent review also lists a variety of passive applications of metasurfaces in absorbers, polarizers, and lenses.[7] Nevertheless, their potential in receiver arrays has not yet been fully explored. In combination with semiconductor bolometers, metamaterials composed of subwavelength size antenna structures can become a novel type of radiation detector that is sensitive to terahertz radiation.[8] While semiconducting electronics have essentially reached their full potential with little room for further improvement, superconducting devices still offer a large amount of potential.

In this study, we develop a metamaterial with highly sensitive bolometers of the Superconductor-Insulator-Normal metal-Insulator-Superconductor (SINIS) type to achieve maximum sensitivity while maintaining a broad spectral bandwidth suitable for receivers intended for radioastronomy.

II. SAMPLE DESIGN AND FABRICATION

We designed and fabricated three different types of a metamaterial building block: with wide [Figs. 1(a) and 1(b)] and narrow [Fig. 1(c)] split-ring antennas each containing two or four bolometers. A wide split-ring antenna with four bolometers [Fig. 1(a)] is intended for a symmetric connection and immersion in a hyperhemisphere lens, and types (b) and (c) for matching with a back-to-back horn. The central frequency for the array can be estimated from the lump element model. By varying the diameter and width of the circle, we change the inductance, while the NIS junction area can be adjusted to obtain the necessary capacitance.

The unit cell [Fig. 1(a)] is similar to a split-ring resonator (SRR) that is generic for many metamaterials. In our design, the ring's outer diameter and width are $2R = 54\,\mu m$ and $2r = 15\,\mu m$, respectively, which yields the following Au film ring inductance:

$$L = \mu_0 R\left[\ln\left(\frac{8R}{r}\right) - 1.75\right] = 54\ \text{pH}.$$

Each of the four SINIS bolometers with 8 NIS $0.8\,\mu m^2$ area junctions connected in series possesses a capacitance of 7 fF, if the specific capacitance of a single NIS junction is $70\ fF/\mu m^2$. As a result, we obtain a lumped tank circuit LC resonant frequency of 260 GHz for individual unit cells. The sum load of eight $30\,\Omega$ normal metal absorbers connected in parallel and series is $R = 60\,\Omega$ which correspond to a rather low quality factor for such a lump element resonator: $Q = \omega L/R = 88/60 = 1.4$.

Successively, the period between unit cells in the matrix needs to be chosen. Usually, metamaterials are designed with the aim to obtain a high Q-factor while providing high frequency selectivity. This is achieved by optimizing the distance between unit cells, so they equal the wavelength in the dielectric substrate, corresponding to radiative interaction of SRRs in the substrate. Laterally coupled SRRs influence the resonance sharpness through lattice modes.[9,10] A similar effect, referred to as Wood anomaly, is observed in quasi-optical filters as a sharp absorption peak in the transmission spectra. If the distance between neighboring SRRs is too large, the external illumination and field from neighboring SRRs are out of phase and they interfere destructively. With smaller distances, the relative phase between the external illumination and scattered radiation from neighbors can be constructive. However, care should be taken as reducing the distance too much can increase capacitive and inductive coupling. The highest Q-factor is obtained for distances that are equal to the resonant wavelengths in the dielectric substrate which occurs due to the confinement or trapping of the electromagnetic field in the array. For the detector array, such a confinement can lead to higher losses and a reduction in receiver efficiency.

Conversely, to obtain a wider bandwidth, we need to enhance the damping of the lattice mode that is radiated in the substrate fields from the SRRs. Destructive interference in the substrate plane leads to higher radiative efficiency. It should also be noted that as opposed to capacitive or inductive coupling, which requires close

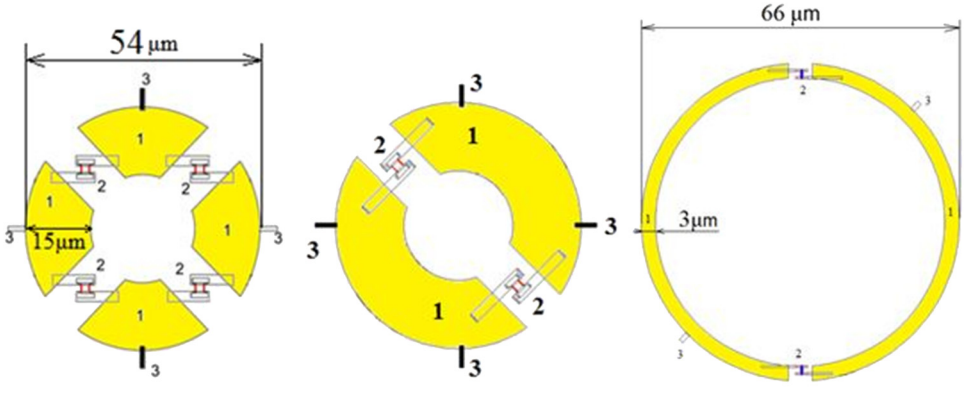

FIG. 1. Designs of unit cells [(a), (b), and (c)] in which (1) are the elements of the split-ring resonator, (2) are the SINIS bolometers, and (3) are the interconnections to neighboring elements; vertical: capacitive contact and horizontal: direct contact.

spacing, radiative coupling is mediated by long-range lattice modes. In the simplest case of two dipole antennas or slot antennas, the optimal interantenna distance is half a substrate wavelength to yield maximal suppression of substrate modes and produce a sharp mainlobe beam pattern in the far field that is perpendicular to the substrate plane. For more complicated configurations of big SRR arrays, the optimal period can only be obtained through numerical modeling. Finally, with our low Q unit cell and a short period of $P \cong \frac{\lambda}{3\sqrt{\epsilon}} \cong 70\,\mu$m, we can expect a rather broadband response for our device that is close to model predictions (Fig. 2 shows the non-symmetric connection). The first mode corresponds to the vertical polarization with a direct connection between rings via interconnection elements (3) in Figs. 1(a)–1(c). The second mode corresponds to the horizontal polarization and exhibits a lower efficiency. The final design was expected to have capacitive horizontal interconnections via horizontal elements (3) with a total series capacitance of the order of 1 pF. In this case, we expect a high efficiency for both polarizations.

We designed and fabricated this metamaterial for the 350 GHz band (Fig. 3). In our earlier work,[11,12] we studied 5×5 matrixes of conventional annular ring antennas for the same 350 GHz band with an outer ring antenna diameter of 300 μm, a width of 20 μm, a period of 475 μm (two wavelengths in the dielectric), covering an area of $2200 \times 2200\,\mu\text{m}^2$. In that case, resonant properties were determined from the distributed half wavelength resonance. Our present metamaterial contains ring antennas with a diameter of 60 μm, a period of 70 μm, and an area of the 10×10 element matrix of $621 \times 621\,\mu\text{m}^2$. As a result, we have a total of 100 antennas within an area of 0.38 mm^2 in the metamaterial matrix. In a conventional matrix,[12] there are only 50 bolometers within a much larger area of 4.8 mm^2. This means that for the same single bolometer saturation power, the metamaterial matrix delivers a power density that is 41 times higher. At the same time, pixels in the imaging array can be placed much closer together thereby delivering a higher angular resolution in the multipixel imaging array.

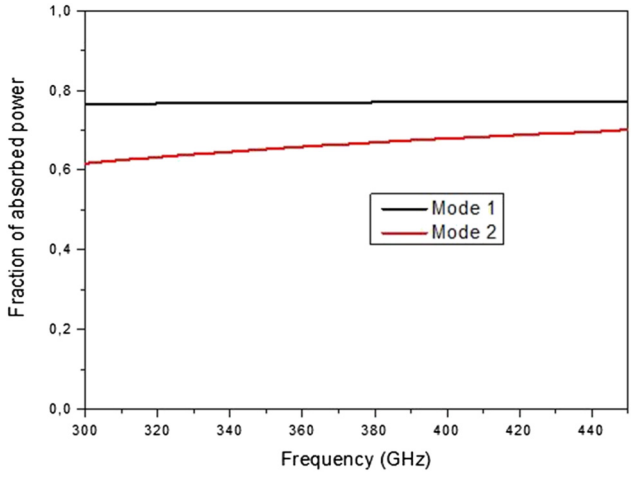

FIG. 2. Absorbed power in a series array, calculated for two polarizations.

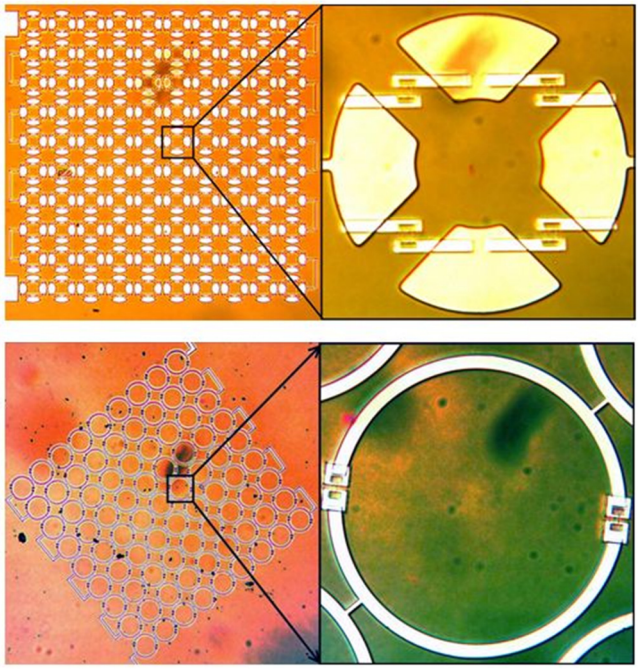

FIG. 3. Metamaterial matrix with a series annular antenna array and a wide circle with four SINIS (top panel); a narrow circle with two SINIS bolometers (bottom panel).

Our metamaterial series array is intended for junction field-effect transistor (JFET) readout. The design parameters for the series connection of bolometers are normal array resistance of around 100 kΩ, a maximum resistance of more than 5 MΩ at 300 mK, and a dynamic resistance at optimal bias point of about 500 kΩ to guarantee suitability for JFET or metal-oxide-semiconductor field-effect transistor (MOSFET) readout.

The optimized fabrication process included just two main steps. The first step included laser lithography, magnetron sputtering of TiAuPd for contact pads, wiring and antennas, and lift-off. The second step included e-beam lithography, shadow evaporation at three angles of FeAl absorber and Al electrodes, and lift-off.

III. EXPERIMENTAL RESULTS

Current-voltage characteristics and responsivity to blackbody radiation were measured in a dilution cryostat[13] across the temperature range of 100–300 mK. Samples were attached to an extended hyper-hemisphere sapphire lens illuminated by a variable temperature blackbody radiation source mounted at the 300 mK temperature stage. Bandpass and low-pass filters were placed between the source and the sample to only allow the proper bandwidth of the incoming radiation to reach the sample (Fig. 4).

The IV curve and the dynamic resistance of the annular antenna array metamaterial (AAAM) sample at 300 mK shows a sum gap of 31 mV, an asymptotic resistance of 150 kΩ, and a maximum dynamic resistance of 5 MΩ. The response to blackbody radiation is

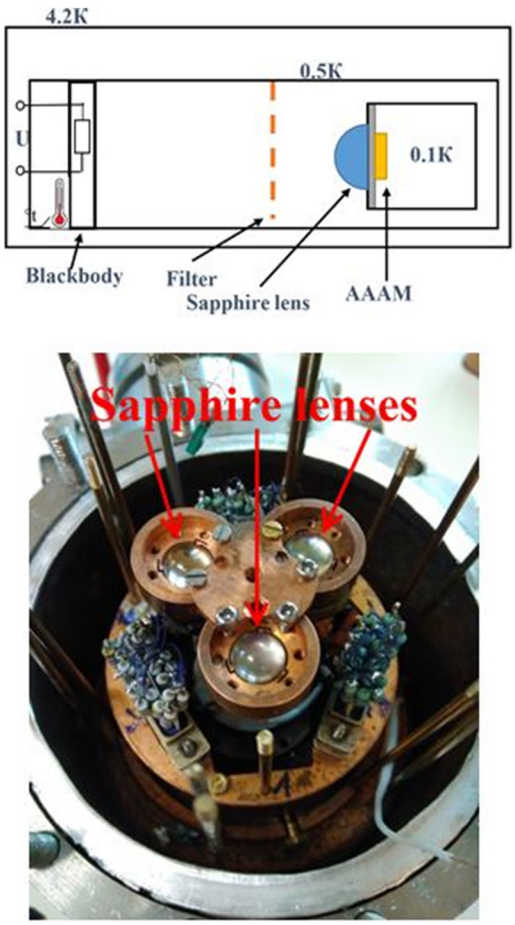

FIG. 4. Simplified schematic of the experiment (top) and a photo of the opened cryostat showing the three sample holders with the three sapphire lenses in the center (bottom).

presented in Fig. 5, and the corresponding responsivity dependence on blackbody temperature in Fig. 6.

We also measured the current and voltage responses for a parallel array of 9×9 annular antennas (Fig. 7). The sample was dc current biased. The voltage pulses of 0.1 s duration with a period of 1 s were applied to the radiation blackbody source. The 1 s periodicity is sufficient to cool the radiation source to equilibrium temperatures. The output signal was integrated using a TEKTRONIX oscilloscope during 128 (or 256) pulses. The instantaneous source temperature was determined by accounting for the thermal capacity of the sapphire substrate and the applied energy. The power of the incoming radiation was calculated for the emitter's maximum temperature. This yielded a current responsivity of 2.4×10^4 A/W.

The spectral response was measured in a He3 sorption cryostat with an optical window that was equipped with neutral density filters at three temperature stages. Numerical simulation results suggest an AAAM spectral response that is quite uniform and wide (Fig. 2). The spectral dependence of the response for a conventional array of

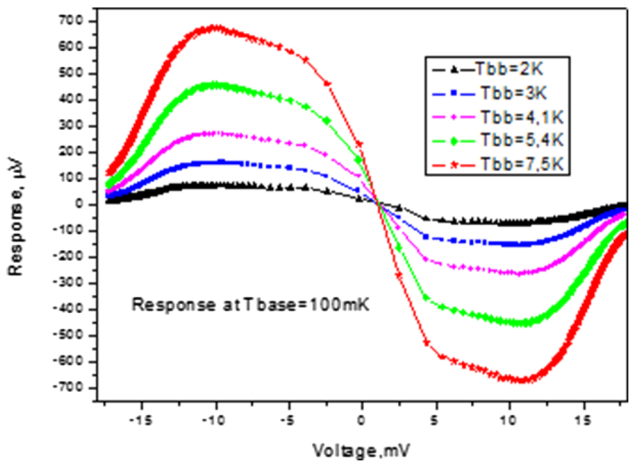

FIG. 5. Voltage response for blackbody radiation source temperatures from 2 K to 7.5 K and a bath temperature of 100 mK.

$300\,\mu$m diameter circular antennas[6] is presented for comparison (Fig. 8). The heterogeneity in the spectral response is partially due to reflections and losses in the optical window and filters. The average absorption by the metamaterial matrix in the given frequency band is at least twice as high in comparison to the half-wave circle matrix.

IV. DISCUSSION

SINIS bolometer performance can be estimated taking into account various parameters: electron-electron, electron-phonon, phonon-phonon interactions, electron cooling, semi-empirical

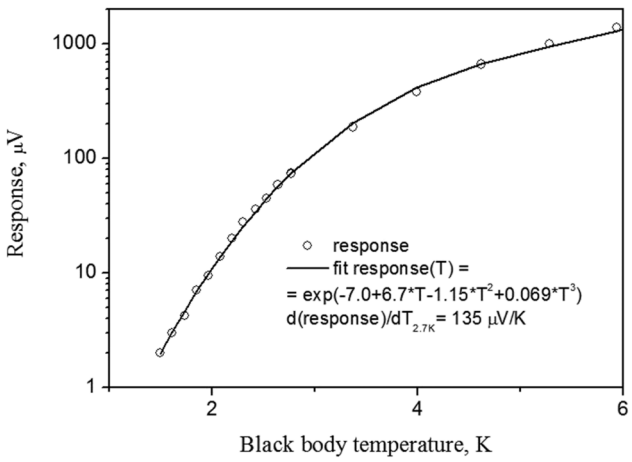

FIG. 6. Voltage responsivity dependence on blackbody source temperature (clear overheating by signal at black body temperature above 3 K). At 2.7 K, the responsivity is $135\,\mu$V/K. For an amplifier noise of 7 nV/Hz$^{1/2}$, this corresponds to a temperature sensitivity of 50 mK/Hz$^{1/2}$ or a relative variation of temperature of 2×10^{-5}.

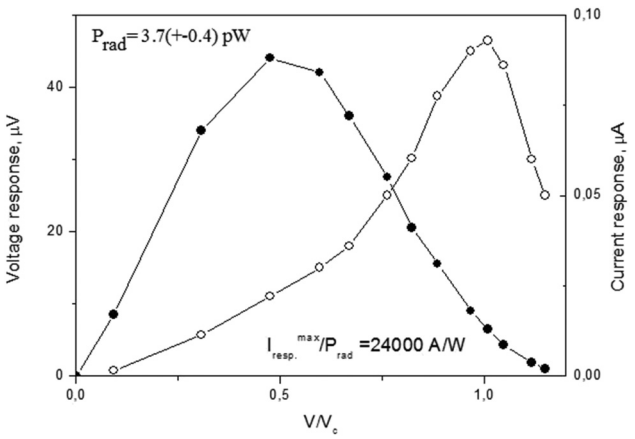

FIG. 7. Voltage response (black circles) and current response (open circles) for our parallel metamaterial matrix, measured at a 100 mK bath temperature and a peak power of 3.7 pW.

Dynes parameter, back-tunneling of hot quasiparticles from superconductor to absorber, etc. Our review of such estimations is presented in Ref. 14. In practice, such modeling with five fitting parameters does not bring a clear understanding of the dynamics of bolometer at different levels of background power load and signal power. Here, we present the analysis of responsivity dependence on applied power with electron-phonon interaction as the main cooling mechanism.

For the relatively high stray background power load, the equivalent electron temperature of the bolometers is above 230 mK, even

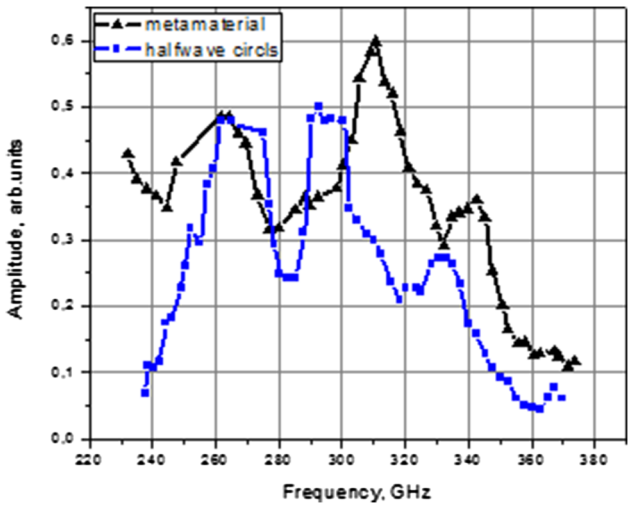

FIG. 8. Spectral response for metamaterial matrix and conventional half-wave circle matrix. Both curves were measured simultaneously with a Backward Wave Oscillator source through a quasi-optical window, three cold neutral density filters, and the same spectrally heterogeneous incoming signal.

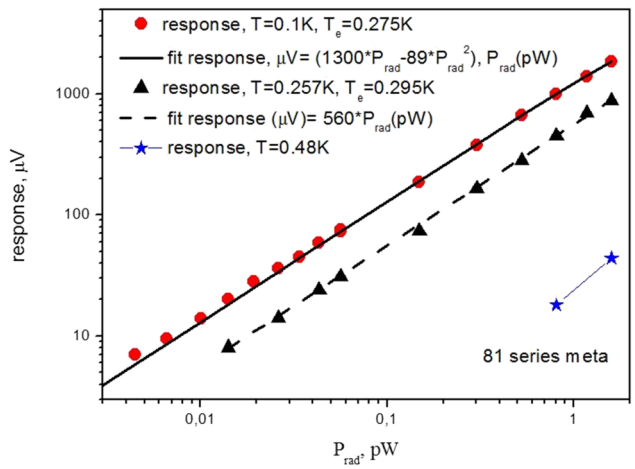

FIG. 9. Voltage response vs blackbody temperature for sample temperatures of 100 mK, 257 mK, and 480 mK. The corresponding electron temperatures are 230 mK, 280 mK, and 480 mK. For low power, the voltage responsivity approaches 1.3×10^9 V/W.

if the sample holder temperature is below 100 mK. In these cases of overheating (Fig. 9), the voltage response is fairly linear. We did not see strong variations in the responsivity dV/dP on the incoming signal power and observe the dynamic range over 30 dB.

In the absence of overheating from the background power and signal, the variations of absorber temperature can be explained from the following electron-phonon interaction relation:

$$P_{sig} = \Sigma v (T_e^5 - T_0^5),$$

where $\Sigma = 3 \times 10^9$ W m^{-3} K^{-5} is a material-specific parameter, v is the absorber volume, T_e is the electron temperature, and T_0 is the phonon temperature. The corresponding thermal conductivity is $G_{ep} = dP/dT_e = 5\Sigma v T_e^4$, from which we can deduce the electron temperature dependence of voltage responsivity:

$$S = \frac{dV}{dP} = \frac{dV}{dT}\cdot\frac{dT}{dP} = \frac{dV}{dT}\frac{1}{G} = \frac{dV}{dT}\cdot\frac{1}{5\Sigma v T^4}. \quad (1)$$

If we use the maximum temperature response for aluminum NIS junctions as $dV/dT = V_\Delta/T_e = 8$ mV/K for the ideal case or $dV/dT = 20\,k/e = 2$ mV/K as the value typically observed in practical applications,[7] this yields a responsivity dependence of $S = 5 \times 10^6/T^4$ for our single bolometer with an absorber volume of 2×10^{-20} m^3. This in turn corresponds to 1.2×10^{10} V/W for an electron temperature of 0.1 K. For a matrix comprised of 100 such bolometers, the absorber volume is 100 times larger and the calculated responsivity estimation drops to 1.2×10^8 V/W. This is only valid, however, as long as we avoid overheating by stray background power. A high signal or background power load absorption will result in significant changes to the electron temperature

that should directly affect responsivity:[7]

$$S_v^{max} = \frac{2k}{e}\frac{1}{(\Sigma v)^{0.2}}\frac{1}{P^{0.8}}. \quad (2)$$

An important feature of this equation is that it does not contain the phonon temperature of the bolometer. Instead, it depends on the electron temperature determined by the absorbed signal power. The current responsivity dependence on the electron temperature is even more pronounced and to a first approximation can be written as $S_i = e/(2kT_e)$.

Now, we can compare the responsivities of a single bolometer and of a series matrix of bolometers exposed to a single-mode radiation at identical blackbody radiation temperatures. We had the following initial parameters: absorber volume for a single bolometer of $v = 0.02\,\mu m^3$, a background radiation power of $P = 1$ pW for a single mode, and an absorber material parameter of $\Sigma = 2 \times 10^9$ W/m^{3}K^5. For a single bolometer, the responsivity should be $S_v = 2 \times 10^8$ V/W. If the power load is reduced by a factor of 10 to 0.1 pW, the responsivity increases to 1.3×10^9 V/W.

For the matrix with $n = 100$ bolometers exposed to the same single-mode input, the signal power in each bolometer is 100 times lower, but due to their series interconnection, the 100 individual output signals are summed. For one bolometer, due to the reduced heating power, the background limited responsivity according to Eq. (2) should be $(100)^{0.8} = 40$ times as high. However, the signal level for each bolometer is 100 times lower, and the sum of the signal from the series array is 100 times higher. As a result, the array total voltage response increases by a factor of 40 compared to a single bolometer. As soon as the signal level exceeds the background power load, both the responsivity and the output signal decrease. In our case, this can happen already at blackbody temperatures over 5 K and a further increase to 10 K leads to a heating power increase to 5 pW and 3.6-fold decline in responsivity. For the case of background limited responsivity, we can also calculate this overheating power for a single bolometer as

$$P_{bg} = \left(\frac{2k}{eS_{max}}\right)^{1.25}\frac{1}{(\Sigma v)^{0.25}}. \quad (3)$$

For a measured array responsivity of $dV_{resparr}/dP_{arr} = 1.3 \times 10^9$ V/W, the corresponding background power for a single bolometer is $P_{sing} = P_{arr}/n$ and the voltage response $V_{respsing} = V_{resparr}/n$, so the responsivity of a single bolometer is $dV_{respsing}/dP_{sing} = dV_{resparr}/dP_{arr}$, i.e., identical to the array responsivity. The background power for a single bolometer is P_{bgarr}/n and the background power for the array can thus be estimated from Eq. (3) as 40 fW for a single bolometer and as $n \times P_{bg} = 4$ pW for the entire array.

V. CONCLUSION

The primary application area of annular antenna array metamaterial with SINIS bolometers is radioastronomy, namely, cosmic microwave background measurements that require high sensitivity and high dynamic range. Such a metamaterial array can be viewed as a distributed absorber with enhanced absorption and bandwidth. Through the use of electrically small antennas in a metamaterial configuration, we were able to construct a matrix that is sufficiently small to fit into the Airy disk of an extended hyper-hemispherical sapphire lens. At a bath temperature of 100 mK and incoming power level in the range of 2–7 pW, the responsivity approaches 1.3×10^9 V/W with a dynamic range of over 30 dB in the case of a power load limited response. The spectral bandwidth is rather uniform in the measured frequency range of 240–370 GHz. The equivalent temperature responsivity at a radiation level of 2.7 K is about $100\,\mu K/Hz^{0.5}$, which makes such devices suitable for measurements of cosmic background radiation anisotropy.

ACKNOWLEDGMENTS

This work was carried out at IREE RAS within the framework of the state task.

REFERENCES

[1]L. J. Chu, "Physical limitations of omni-directional antennas," J. Appl. Phys. **19**, 1163 (1948).
[2]T. J. Yen, W. J. Padilla, N. Fang, D. C. Vier, D. R. Smith, J. B. Pendry, D. N. Basov, and X. Zhang, "Terahertz magnetic response from artificial materials," Science **303**(5663), 1494–1496 (2004).
[3]M. Gupta, Y. K. Srivastava, M. Manjappa, and R. Singh, "Sensing with toroidal metamaterial," Appl. Phys. Lett. **110**, 121108 (2017).
[4]C. Zhang, Q. Cheng, J. Yang, J. Zhao, and T. J. Cui, "Broadband metamaterial for optical transparency and microwave absorption," Appl. Phys. Lett. **110**, 143511 (2017).
[5]N. I. Landy, S. Sajuyigbe, J. J. Mock, D. R. Smith, and W. J. Padilla, "Perfect metamaterial absorber," Phys. Rev. Lett. **100**, 207402 (2008).
[6]A. Li, E. Forati, and D. Sievenpiper, "Study of the electric field enhancement in resonant metasurfaces," J. Opt. **19**, 125104 (2017).
[7]A. Li, S. Singh, and D. Sievenpiper, "Metasurfaces and their applications," Nanophotonics **7**(6), 989–1011 (2018).
[8]J. Grant, I. Escorcia-Carranza, C. Li, I. McCrindle, J. Gough, and D. Cumming, "A monolithic resonant terahertz sensor element comprising a metamaterial absorber and micro-bolometer," Laser Photonics Rev. **7**(6), 1043–1048 (2013).
[9]A. Bitzer, J. Wallauer, H. Helm, H. Merbold, T. Feurer, and M. Walther, "Lattice modes mediate radiative coupling in metamaterial arrays," Opt. Express **17**(24), 22108–22113 (2009).
[10]R. Singh, C. Rockstuhl, and W. Zhang, "Strong influence of packing density in terahertz metamaterials," Appl. Phys. Lett. **97**, 241108 (2010).
[11]S. Mahashabde, A. Sobolev, G. Tsydynzhapov *et al.*, "Planar frequency selective bolometric array at 350 GHz," IEEE Trans. Terahertz Sci. Technol. **5**(1), 37–43 (2015).
[12]S. Mahashabde, A. Sobolev, A. Bengtsson *et al.*, "A frequency selective surface based focal plane receiver for the OLIMPO balloon-borne telescope," IEEE Trans. Terahertz Sci. Technol. **5**(1), 145–152 (2015).
[13]V. S. Edelman, "A dilution microcryostat-insert," Instrum. Exp. Tech. **52**(N2), 301–307 (2009).
[14]M. Tarasov and V. Edelman, "Nanodevices with normal metal–insulator–superconductor tunnel junctions," in *Functional Nanostructures and Metamaterials for Superconducting Spintronics*, NanoScience and Technology, edited by A. Sidorenko (Springer, Cham, 2018), pp. 91–116, ISBN 978-3-319-90481-8.